

Pulse-oximetry accurately predicts lung pathology and the immune response during influenza infection

David Verhoeven, John Teijaro, and Donna L. Farber

**Department of Surgery
University of Maryland School of Medicine
Baltimore, MD 21210**

Keywords: Influenza, lung, viral immunity, pulse-oximetry, immunodeficiency, immunopathology

Corresponding Author: Donna L. Farber, Ph.D., Department of Surgery, University of Maryland School of Medicine, MSTF Building, Room 400, 685 W. Baltimore ST. Baltimore, MD 21201
Phone: 410-706-7458; FAX: 410-706-0311; e-mail: dfarber@smail.umaryland.edu

ABSTRACT

In animal models of influenza, systemic weight-loss is the primary indicator of morbidity from infection, which does not assess local lung pathology or the immune response. Here, we used a mouse-adapted pulse-oximeter as a non-invasive clinical readout of lung function during influenza infection in mice, and found direct correlations between oxygen saturation levels and lung pathology, that reflected the morbidity and survival from influenza infection. We found blood oxygen levels to be a more accurate assessment than weight-loss morbidity in predicting lung pathology in hosts infected with different viral doses, and in assessing immune-mediated viral clearance in the lung.

INTRODUCTION

Respiratory virus infections such as influenza trigger inflammatory responses both systemically and at the site of infection in the lung. The systemic release of inflammatory cytokines from host immune cells is associated with weight-loss morbidity in animal models of influenza (La Gruta, 2007), and with mortality in humans infected with the pandemic 1918 influenza and avian influenza (H5N1) strains (Hsieh, 2006). In the lung, influenza infection leads to virus-associated epithelial damage, and to local immune and inflammatory responses leading to pneumonia (Taubenberger, 2008). The contribution of systemic and local lung responses to influenza morbidity, and the predictive value of measuring systemic versus local lung responses in determining the outcome of influenza infection have not been established.

The “gold-standard” of evaluating morbidity in murine models of viral disease including influenza, is measuring the percentage of body weight lost during the course of infection (Mozdzanowska, 2005; van der Laan, 2008). However, weight loss is not a reliable predictor of infection outcome or survival as mice can readily recover losses of 25-30% of body weight. Moreover, it is not known how weight loss correlates with the extent of lung pathology and the lung-specific immune response. Pulse-oximetry provides a measure of lung function and blood oxygenation determined by spectrophotometric analysis of the percent of oxygenated hemoglobin (Wahr, 1995). In humans, pulse-oximeters provide an important clinical readout of morbidity in respiratory diseases; however, human pulse-oximeters have not been readily adapted to analyze animal models of disease (Sidwell, 1992).

In this study, we hypothesized that morbidity and outcome of influenza virus infection could be better predicted by measuring lung function parameters compared to systemic weight loss. We used a newly developed pulse-oximeter adapted for use in rodents, to follow the progress of

influenza infection according to variations in viral load and host immune status. We found that SpO₂ levels directly correlated with lung pathology at all stages of infection, and allowed more fine-tuned assessment of the effect of viral dose on outcome compared to weight loss parameters alone. In addition, we found that SpO₂ levels were proportional to the efficacy of the immune response in immunodeficient mice and in mice presensitized to influenza, where weight-loss failed to predict infection outcome. Our results indicate that SpO₂ levels provide a valuable non-invasive assessment of lung function and pathology, and a superior predictor of morbidity and mortality from respiratory viral disease.

RESULTS

Oxygen saturation levels and initial infectious dose

To assess whether oxygen saturation levels in the blood could be useful indicators of the severity of influenza infection, we infected BALB/c mice intranasally with increasing doses from 10-1000 TCID₅₀ of influenza A/PR8/34 (PR8) virus, and assessed both weight loss and SpO₂ levels during the course of infection. We previously determined that doses of 10 TCID₅₀ and 100 TCID₅₀ were sub-lethal infectious doses with full recovery of weight loss within 10-14 days post-infection, while ≥ 1000 TCID₅₀ constituted a lethal dose (2LD₅₀), with mortality occurring within 15 days post infection (data not shown). Measurements of weight-loss during the course of infection showed that mice infected with a 10 TCID₅₀ dose lost only a moderate amount of weight and began to recover weight after day 7 post-infection, reaching the starting weight by day 9 post-infection. By contrast, mice infected with 100 or 1000 TCID₅₀ doses both exhibited similar precipitous weight loss of 30% of their starting weight by day 8 post-infection, after which responses to these two infectious doses diverged. Whereas 100 TCID₅₀-infected mice beginning to recover weight at day 10 post-infection, 1000 TCID₅₀-infected mice lost additional weight falling to <70% of their starting weight, which remained low throughout the infection period (day 12 post-infection) (Fig 1A).

We examined how viral replication correlated to weight loss in the differentially infected mice by assessing lung viral titers at day 5 post-infection representing the peak of viral replication, day 7 representing the initial drop in viral titers, and day 12 representing the clearance stage of viral replication (Jelley-Gibbs, 2007). At day 5, the lung viral titers were proportional to the initial viral doses with mice infected with 10 TCID₅₀ of PR8 having the lowest viral titers, followed by 100 TCID₅₀-infected mice, with 1000 TCID₅₀-infected mice having the highest lung viral load that was 50 fold higher than mice infected with 100 TCID₅₀ (Fig 1B). At day 7 post-infection, lung viral

titers in the 100 and 1000 TCID₅₀-infected mice were still 4 orders of magnitude greater than viral loads in 10 TCID₅₀-infected mice which had already cleared the majority of the virus. However, by day 12 post-infection, virus could not be detected in the lungs of all infected groups indicating viral clearance (Fig. 1B). These results show that while the peak viral load in the lung was proportional to the initial infectious dose, the kinetics of complete viral clearance was similar in mice receiving both sublethal and lethal influenza doses.

The disparities between weight loss, viral dose and viral titers at different timepoints emphasized the need for additional readouts of clinical outcome during influenza infection. We evaluated oxygen saturation levels in each mouse group receiving different infectious doses at intervals from day 0-12 post-infection using the rodent-adapted pulse oximeter (Starr Life Sciences). Mock infected mice maintained near 100% SpO₂, as expected, as any decrease in SpO₂ less than 95% is considered grave in human patients (Wahr, 1995). Influenza-infected mice at all doses exhibited marked decreases in SpO₂ levels starting at day 3 until day 7 post- with the reduction in SpO₂ level proportional to the infectious dose. At day 7 post-infection, 10 and 100 TCID₅₀-infected mice exhibited 93% and <90% SpO₂, respectively, with 1000 TCID₅₀-infected mice having <85% SpO₂ indicating severe hypoxia (Fig. 1C). These results demonstrate that at day 7 post-infection, when the difference in weight loss and viral titers was not significant between 100 and 1000 TCID₅₀-infected mice, SpO₂ levels were more accurate indicators of the lung viral load.

At later timepoints post-infection, SpO₂ levels were particularly informative with regards to recovery from infection after virus was cleared. By day 12 post-infection when virus was cleared in all groups, both 10 and 100 TCID₅₀ infected mice still maintained lower SpO₂ than pre-infection levels with 10 TCID₅₀ having 95% and 100 TCID₅₀-infected exhibiting SpO₂ levels <94% (Fig 1C), despite having recovered most of their starting weight. SpO₂ levels were dramatically decreased in

1000 TCID₅₀-infected mice to <80% at 12 days post-infection, indicating severe hypoxia and irreversible morbidity (Fig. 1C), and consistent with continued weight-loss. These results indicate that SpO₂ measurements can provide an assessment of continuing pathological damage in the lung after virus is cleared although mice are recovering weight.

Oxygen saturation levels indicate lung pathology

The results above suggested that SpO₂ measurements may indicate the level of lung pathology. We therefore analyzed pathology in lung tissue sections obtained from mice infected with different doses of influenza at 5, 7 and 12 days post-infection (Fig. 2). At day 5 post-infection, mice that received 10 TCID₅₀ exhibited desquamation of the alveolar epithelium in response to virus infection (Fig 2A) with minimal leukocyte infiltration into interstitial tissues and minimal lung consolidation as compared to uninfected controls (Fig 2J). Leukocyte infiltration and lung consolidation increased by day 7 post-infection in 10 TCID₅₀-infected mice (Fig 2D), but was resolved at day 12 post-infection (Fig 2G) when lung architecture resembled uninfected controls with the exception of small, dispersed regions within the interstitial tissue. In 100 TCID₅₀-infected mice, increased leukocyte infiltration was observed at day 5 post-infection with mild disruption of normal alveoli structure compared to uninfected or 10 TCID₅₀-infected mice. The observed pathology in 100 TCID₅₀-infected mice increased through day 7 post-infection with an greater number of occluded alveolar spaces (Fig 2E), and by day 12 post-infection there were some alveolar epithelium that continued to exhibit desquamation along with areas that returned to normal morphology (Fig 2H). Mice infected with 1000 TCID₅₀ exhibited more intensive leukocyte infiltration with condensation appearing around the bronchioles and epithelial sloughing within the larger airways and alveoli compared to the other groups at 5 days post-infection (Fig 2C). The level of infiltration and consolidation coincident with alterations in alveolar architecture continued to

increase by day 7 post-infection (Fig 2F) exhibiting the most severe pathology at day 12 post-infection (Fig 2I), when the lungs were heavily consolidated with minimal normal lung architecture. These results demonstrate that the observed oxygen saturation levels not only matched the early viral replication detected in each group, but also appeared to better correlate with the actual pathology in the lung tissue even after viral clearance.

Effect of temperature on peripheral oxygen saturation levels

Because pulse-oximetry readings depend on the level of blood flow which can be altered by temperature, and influenza infection in mice has been shown to lead to a temperature drop (Jhaveri, 2007), we compared SpO₂ levels in lethally challenged mice (1000 TCID₅₀) prior to and after application of systemic or locally applied heat. As compared to uninfected mice, influenza infection resulted in decreased body temperature (average of 3.8°C) and average SpO₂ of 79%. Heating of mice to raise their body temperature to the level of uninfected controls, resulted in slightly increased levels of oxygen saturation levels to an average of 83.3%, that was not statistically different from unheated infected mice (Table 1). To limit the effects of vasodilatation in the lungs contributing to increased oxygen saturation after systemically applied heating, heat packs were applied to the leg used to measure oxygen saturation. We determined that three minutes of direct warming to the leg led to vasodilatation in saphenous veins (data not shown). As shown in Table 1, lethally challenged mice (1000 TCID₅₀) had no change in the SpO₂ levels after heating (80.2%) compared to SpO₂ levels prior to heating (80%). These data demonstrate that the decreased SpO₂ levels observed in influenza- infected mice are not appreciably altered by warming.

Oxygen saturation as a non-invasive readout of the immune response

The immune response to influenza infection determines the outcome of infection, by providing viral clearance in the lung, contributing to the systemic inflammatory response, and also

can promote immunopathology. We asked whether SpO₂ would also provide a more accurate readout for the efficacy of the host immune response driving viral clearance in the lungs. We assessed weight loss, viral load, and SpO₂ measurements in intact naive mice at the 100 TCID₅₀ dose compared to a similar infectious dose in RAG2-deficient (RAG2^{-/-}) mice lacking an adaptive immune response, and mice that received influenza-specific memory T cells obtained from mice which were previously infected and had cleared an influenza infection. With these groups, we could determine the contribution of the innate immune system or adaptive memory responses to weight loss and oxygen saturation levels after infection. Interestingly, RAG2^{-/-} mice lost the least amount of weight as compared to infected naive and memory mice both of which exhibited comparable weight-loss morbidity up to day seven post-infection (Fig. 3A). These relative weight loss measurements did not correlate to the viral load in these mouse groups. Compared to the viral loads in 100 TCID₅₀-infected intact mice, RAG2^{-/-} mice exhibited the highest viral loads in the lung, consistent with their lack of an adaptive immune response that results in eventual death by viremia (Bot A, 1996), and mice with memory T cells had the lowest viral loads (Fig. 3C), consistent with the ability of memory T cells to mediate protective immunity.

Interestingly, SpO₂ levels measured by pulse-oximetry exhibited an inverse correlation with viral loads in the lung. SpO₂ in infected RAG2^{-/-} mice followed a similar precipitous decline observed in intact mice infected with a lethal dose of influenza, decreasing to near 80% at 7 days post-infection (Fig. 3B), consistent with the high viral loads. Mice with influenza-specific memory T cells maintained higher SpO₂ levels at all time-points post-infection compared to that of naive infected mice (Fig. 3B), consistent with their enhanced viral clearance. When taken together, assessing multiple parameters during influenza infection reveals that SpO₂ levels provide an accurate indicator of the efficacy of the immune response, whereas weight loss measurements did

not reflect the ability of mice differing in immune status to clear the infection. In the case of RAG2^{-/-} immune-deficient mice, the lack of substantial weight-loss morbidity was paradoxical with the high viral load and poor outcome, and the rapid weight loss of mice with preformed memory T cell immunity to influenza did not accurately reflect the increased viral clearance in these mice.

To assess whether SpO₂ levels likewise indicated the level of lung pathology in immune competent versus immune-deficient mice, we compared lung sections stained by H&E in 100 TCID₅₀ infected intact mice and RAG2^{-/-} mice at 7 days post-infection. As before, we found that intact mice infected with 100 TCID₅₀ had moderate levels of leukocyte infiltration, disruption of normal alveolar architecture, and mild lung consolidation (Fig 3D, top). In stark contrast, influenza-infected RAG2^{-/-} mice had severe lung consolidation throughout most of the tissue and extensive infiltration of polynuclear and mononuclear leukocytes which occluded the airway architecture (Fig. 3D, bottom). These results show that SpO₂ levels served as accurate indicators of the severity of lung pathology as well as viral clearance in mice of different immune status, whereas weight loss measurements did not reflect the lung-specific response.

DISCUSSION

The outcome of respiratory viral infections such as influenza depends on multiple parameters including the extent of virus-associated pathology in the lung, and the local and systemic immune and inflammatory response. Treating established infections will require knowledge of the pathogenesis of infection and the extent of inflammation and immunopathology. Currently, readouts of infection in animal models rely chiefly on systemic weight-loss measurements to indicate virus-induced morbidity and predict infection outcome. Here, we used a pulse-oximeter adapted for use in mice to assess how oxygen saturation levels could serve as an indicator and predictor of the outcome of influenza infection. Our results demonstrate that measurement of SpO₂ by pulse-oximetry accurately reflects the pathologic conditions in the lung during viral infection and is a reliable indicator of the efficacy of the host immune response in the lung. By contrast, weight-loss measurements did not correlate with differences in viral load prior to clearance and were ineffective in predicting the pathology in the lungs during infection.

Measuring oxygen saturation is a reliable and consistent tool that is superior to other systems due to its ease of application and reproducibility. Although sacrificing animals with a weight loss of >25% of initial starting weight is typically utilized in murine models of respiratory infections and generally predicts animals that will not survive infection, mice with pre-existing memory T cells to influenza exhibited a significant weight loss, yet controlled viral replication. Therefore, weight loss alone does not predict the severity of influenza infection but when used in conjunction with oxygen saturation, a better assessment of morbidity and mortality can be obtained. Traditional approaches to monitor lung function in mice using plethysmography to assess bronchial resistance to oxygen diffusion can be inaccurate (Bates, 2004) and thus are not adaptable as reliable predictors of disease outcome.

Influenza infection drives a strong adaptive immune response that not only acts to clear virus, but can also result in immunopathology either systemically through the release of inflammatory mediators, and/or locally through the recruitment of immune effectors to the lung. The limited amount of weight loss observed in the RAG2^{-/-} mice, as compared to infected BALB/c mice, indicates that weight loss pathology is associated with an adaptive response to infection, that has also been shown in other models such as RSV, murine pneumonia virus, and metapneumovirus with secondary bacterial infections (Bueno, 2008; Frey, 2008; Kukavica-Ibrulj, 2009). Indeed, mortality from pandemic strains of influenza has been attributed to an overzealous immune response (Kash, 2006). Here, we demonstrate lung immunopathology following viral clearance, particularly in mice infected with higher viral doses. Paradoxically, the lowest SpO₂ levels in 1000 TCID₅₀-infected mice were observed after viral clearance, suggesting an immune response correlate to lung damage. It has been shown that following influenza infection of mice, antigen depots persist in the lung and lymphoid tissue (Jelley-Gibbs, 2007; Zammit, 2006), which may continue to drive immune activation leading to continued lung inflammation as seen here in all infected groups. SpO₂ levels can accurately indicate immunopathology in the lung long after virus is cleared, with important implications for using mouse models to design therapeutic interventions for treating the deleterious consequences of the immune response to viral infections.

SpO₂ readings clearly and strikingly followed the level of pathology in the lungs and the immune response demonstrating its utility for assessing the amount of lung inflammation without having the need for sacrificing animals during early infection time-points. Since respiratory viral infections can cause significant pathology in the lungs of murine models of infection, measuring oxygen saturation should prove to be an optimal tool for correlating virus titers and lung pathology and obtaining a better assessment for modeling viral infections in murine models.

MATERIALS AND METHODS

Mice.

BALB/c female mice 6 weeks of age were purchased from the National Cancer Institute Biological Testing Branch and housed at the animal facility at the University of Maryland School of Medicine. RAG2^{-/-} mice on BALB/c background (Taconic Farms, Germantown, MD) were bred and maintained at the animal facility. All animal procedures were approved by the Institutional Animal Care and Use committee at University of Maryland, Baltimore.

Influenza infection of mice.

Influenza virus strain A/PR8/34 was grown in the allantoic fluid of chicken eggs as described (Gerhard, 1976). Intranasal infection of mice with doses from 10-1000 TCID₅₀ was performed on anesthetized mice. To generate influenza-specific memory T cells, mice were infected with 100 TCID₅₀ of influenza and allowed to recover. T cells were isolated by negative selection from the spleens of these mice 10 weeks post-infection, and transferred (2×10^6 cells/mice) intravenously into BALB/c hosts and challenged with 100 TCID₅₀ of influenza A/PR8/34 one day after cell transfer.

Oxygen Saturation measurements.

Pulse oximeter (StarLife Sciences, Pittsburg PA) was use to measure blood SpO₂ on mice three and seven days post-infection. Mice were held by hand and the pulse oximeter clip was placed on the hind leg. Mice were held and covered by the light blocker fabric supplied by the manufacturer and held until calm (several seconds), before placing the probe on the hind leg over the skin near the femur bone. In some cases, removal of the hair on the hind legs by shaving or the use of a depilatory agent was necessary to achieve 100% oxygen saturation levels in uninfected mice (data not shown). Three minute readings were taken from each mouse, sorted by spreadsheet for only readings that had no error codes in a block, and the average of 25-50 individual readings were

calculated. In additional experiments, the entire body of mice were heated for three minutes with a heat lamp or a heat pack (HeatMax) was applied directly to the leg of mice for three minutes before immediately reading oxygen saturation levels.

Influenza viral titer measurement

Viral titers were assayed using the MDCK killing assay as described (Gerhard, 1976). MDCK cells were plated to 85% confluency the day before titer determination. Lung tissue from snap frozen tissue of equal weight was serial diluted in DMEM. MDCK were infected for two hours, washed twice, and DMEM containing 0.5% bovine serum albumin (Sigma) and 1ug/ml of trypsin-TPK was added to each well. Three days post-infection, supernatants were harvested and virus quantified by HAI assay (Gerhard, 1976).

Immunohistochemistry

The left lobes of the lungs from infected mice were perfused with 4% formalin and then dissected and immersed in formalin. Five μ M sections of lungs were stained with H&E, and examined by light microscopy.

Statistics

ANOVA analysis or Student T-tests were used to compare each group using a confidence interval of 95%. Mann-Whitney U Test was used to compare oxygen saturation before and after heating using a confidence interval of 95%.

ACKNOWLEDGEMENTS

This work was supported by NIH AI077029 and NIH AI050632 awarded to D.L.F. D.V. was supported by NIH T32 ES007263.

REFERENCES

- Bates J, I. C., Brusasco V, Drazen J, Fredberg J, Loring S, Eidelman D, Ludwig M, Macklem P, Martin J, Milic-Emili J, Hantos Z, Hyatt R, Lai-Fook S, Leff A, Solway J, Lutchen K, Suki B, Mitzner W, Paré P, Pride N, Sly P (2004). The use and misuse of Penh in animal models of lung disease. *American Journal of Respiratory Cell and Molecular Biology* 31(3), 373-374.
- Bot A, R. A., Isobe H, Bot S, Schulman J, Yokoyama WM, Bona CA (1996). Cellular mechanisms involved in protection and recovery from influenza virus infection in immunodeficient mice. *Journal of Virology* 70(8), 5668-5672.
- Bueno SM, G. P., Cautivo KM, Mora JE, Leiva ED, Tobar HE, Fennelly GJ, Eugenin EA, Jacobs WR Jr, Riedel CA, Kalergis AM (2008). Protective T cell immunity against respiratory syncytial virus is efficiently induced by recombinant BCG. *Proceedings of the National Academy of Sciences* 105(52), 20822-20807.
- Frey S., K. C., Schmitt-Graff A, Ehl S. (2008). Role of T cells in virus control and disease after infection with pneumonia virus of mice. *Journal of Virology* 82(23), 116190-11627.
- Gerhard, W. (1976). The analysis of the monoclonal immune response to influenza virus. II. The antigenicity of the viral hemagglutinin. *J Exp Med* 144(4), 985-95.
- Hsieh YC, W. T., Liu DP, Shao PL, Chang LY, Lu CY, Lee CY, Huang FY, Huang LM. (2006). Influenza pandemics: past, present and future. *Journal Formosan Medical Association* 105(1), 1-6.
- Jelley-Gibbs DM, D. J., Brown DM, Strutt TM, McKinstry KK, Swain SL (2007). Persistent depots of influenza antigen fail to induce a cytotoxic CD8 T cell response. *Journal of Immunology* 178(12), 7563-7570.
- Jhaveri KA, T. R., Toth LA. (2007). Effect of environmental temperature on sleep, locomotor activity, core body temperature and immune responses of C57BL/6J mice. *Brain Behavior and Immunology* 21(7), 975-987.
- Kash JC, T. T., Proll SC, Carter V, Perwitasari O, Thomas MJ, Basler CF, Palese P, Taubenberger JK, García-Sastre A, Swayne DE, Katze MG. (2006). Genomic analysis of increased host immune and cell death responses induced by 1918 influenza virus. *Nature* 443:578-581.
- Kukavica-Ibrulj I, H. M., Prince GA, Gagnon C, Bergeron Y, Bergeron MG, Boivin G. (2009). Infection with human metapneumovirus predisposes mice to severe pneumococcal pneumonia. *Journal of Virology* 83(3), 1341-1349.

- La Gruta NL, K. K., Stambas J, Doherty PC. (2007). A question of self-preservation: immunopathology in influenza virus infection. *Immunology and Cell Biology* 85(2), 85-92.
- Mozdzanowska K, F. M., Zharikova D, Feng J, Gerhard W. (2005). Roles of CD4+ T-cell-independent and -dependent antibody responses in the control of influenza virus infection: evidence for noncognate CD4+ T-cell activities that enhance the therapeutic activity of antiviral antibodies. *Journal of Virology* 79(10), 5943-5951.
- Sidwell RW, H. J., Gilbert J, Moscon B, Pedersen G, Burger R, Warren RP (1992). Utilization of pulse oximetry for the study of the inhibitory effects of antiviral agents on influenza virus in mice. *Antimicrobial Agents and Chemotherapy* 36(2), 473-476.
- Taubenberger JK, M. D. (2008). The pathology of influenza virus infections. *Annual Reviews in Pathology* 3, 499-522.
- van der Laan JW, H. C., Lambkin-Williams R, Boyers A, Mann AJ, Oxford J (2008). Animal models in influenza vaccine testing. *Expert Reviews of Vaccines* 7(6), 783-793.
- Wahr JA, T. K., Diab M. (1995). Pulse Oximetry. *Respiratory Care Clinics of North America* 1(1), 77-105.
- Zammit DJ, T. D., Klonowski KD, Lefrançois L, Cauley LS. (2006). Residual antigen presentation after influenza virus infection affects CD8 T cell activation and migration. *Immunity* 24(4), 439-449.

FIGURE LEGENDS

Fig. 1. Oxygen saturation levels correlate with the amount of viral replication in the lungs in murine models of influenza infection. BALB/c mice were infected with 0,10,100, or 1000 TCID₅₀ of influenza strain A/PR8/34 and monitored for weight loss, oxygen saturation and viral titers for a 12 day infectious period. (A) Graph shows percent of starting weight of mice infected with 10, 100 or 1000 TCID₅₀ of influenza from 1-7 days post-infection. (B) Influenza replication was measured by MDCK assay at day 5, day 7, and day 12 post-infection in mice infected with different influenza doses. Significant differences were found at day 3 post-infection indicated by * (p=0.03) and day 7 post-infection indicated by ** (p=0.02) (n=10, +/- SE). (C) Graph shows oxygen saturation levels (SpO₂) as determined by pulse-oximetry (see methods) at day 3 and 7 post-infection. Significant differences were found for groups at day 3 post-infection indicated by * (p<0.001), day 5 post-infection indicated by ** (p<0.001), day 7 post-infection indicated by *** (p=0.003), day 12 post-infection indicated by **** (p<0.001). (Each value is an average ± SE of values from two experiments, n=5 per group per experiment).

Fig. 2. Oxygen saturation levels mirrors the level of lung pathology during influenza infection. H&E staining of lungs of mice infected with (A) 10 TCID₅₀ infected BALB/c mice, (B) 100 TCID₅₀, or (C) 1000 TCID₅₀, at five days post-infection as compared to mice infected with (D) 10 TCID₅₀, (E) 100 TCID₅₀, (F) and 1000 TCID₅₀ at seven days post-infection or with the lungs of (G) 10 TCID₅₀, (H) 100 TCID₅₀, and (I) 1000 TCID₅₀ infected mice at 12 days post-infection as compared to uninfected controls (J). One representative animal of five is shown for each group.

Fig. 3. Immune response suppression of viral replication leads correlates with levels of oxygen saturation. Naive BALB/c mice ("Naive"), RAG2^{-/-} mice, and BALB/c mouse recipients of influenza-primed memory T cells ("Memory") were infected with 100TCID₅₀ of influenza strain A/PR8/34 and monitored as in Fig. 1. (A) Graph shows percent of starting weight of naive, RAG2^{-/-} and memory mice infected with 100 TCID₅₀ influenza from 1-7 days post-infection. (Data are compiled from two experiments of n=5 per group per experiment +/- SE) (B) Lung viral titers in the different mouse groups as determined by the MDCK killing assay at seven days post-infection (n=10,+/- SE). Significant differences were found between all three groups indicated by * (p=0.03). (C) Oxygen saturation levels (SpO₂) as determined by pulse-oximetry at Day 3 and 7 post-infection. Significant differences were found for groups at day 3 post-infection indicated by * (p<0.001), and at Day 7 post-infection indicated by ** (p=0.007). (D) H&E staining of lungs from naive mice (top) and RAG2^{-/-} mice (bottom) infected with 100 TCID₅₀ of PR8 influenza at seven days post-infection. A representative animal is shown for each group.

Table 1: Effect of warming on pulse-oximetry readings in influenza infected mice

<u>Total body Warming:</u> Mouse^a	Rectal Temperature Pre/Post Heat	SpO₂ before heating	SpO₂ after Heating *p=0.08
1	32.2/37.6	79%	83%
2	33.7/36.8	81%	86%
3	32.5/36.1	73.1%	75%
4	33.9/37.6	79.6%	86%
5	32.6/35.0	82.5%	85.6%
<u>Direct application of</u> <u>heat to leg:</u> Mouse^b	Rectal Temperature	SpO₂ before heating	SpO₂ after Heating *p=0.45
1	33.8	82%	83%
2	32.5	81%	79%
3	33.06	76%	74%
4	32.6	81%	85%

^a Mice were warmed under a heating lamp for 3 min., and pulse-oximetry readings taken prior to and following heating

^b Heating pads were applied to the leg and warmed for 3 mins., and pulse-oximetry readings taken prior to and following heating.

Figure 1
Verhoeven, et al

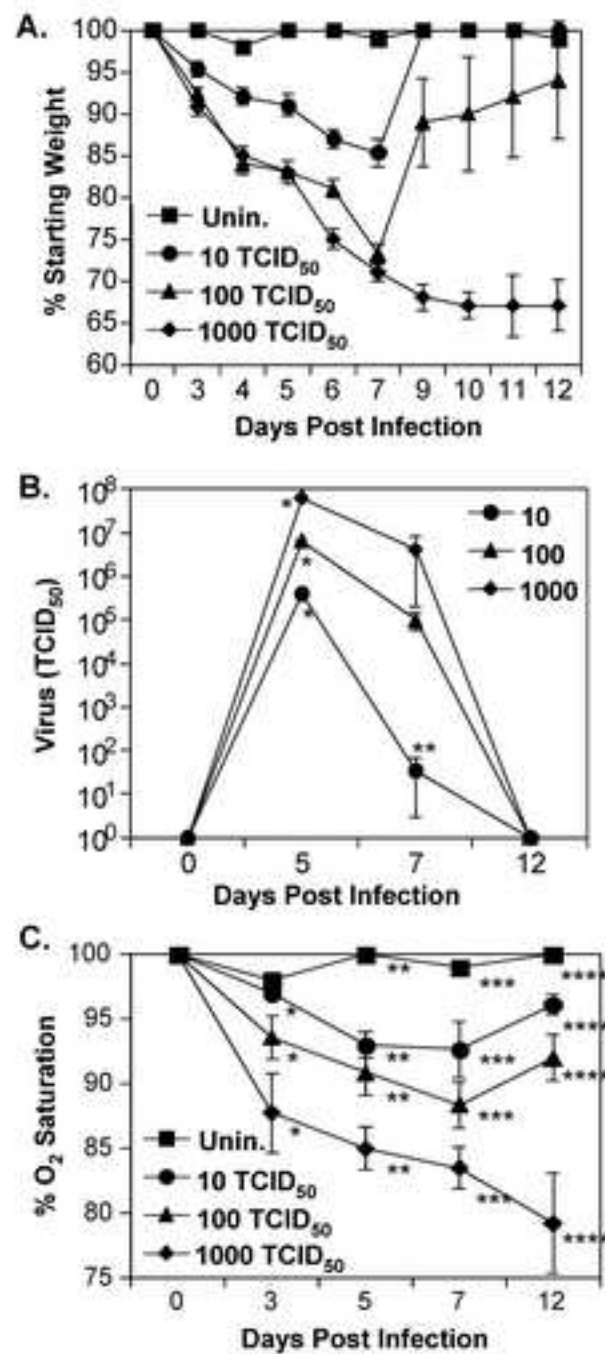


Figure 2
Verhoeven, et al

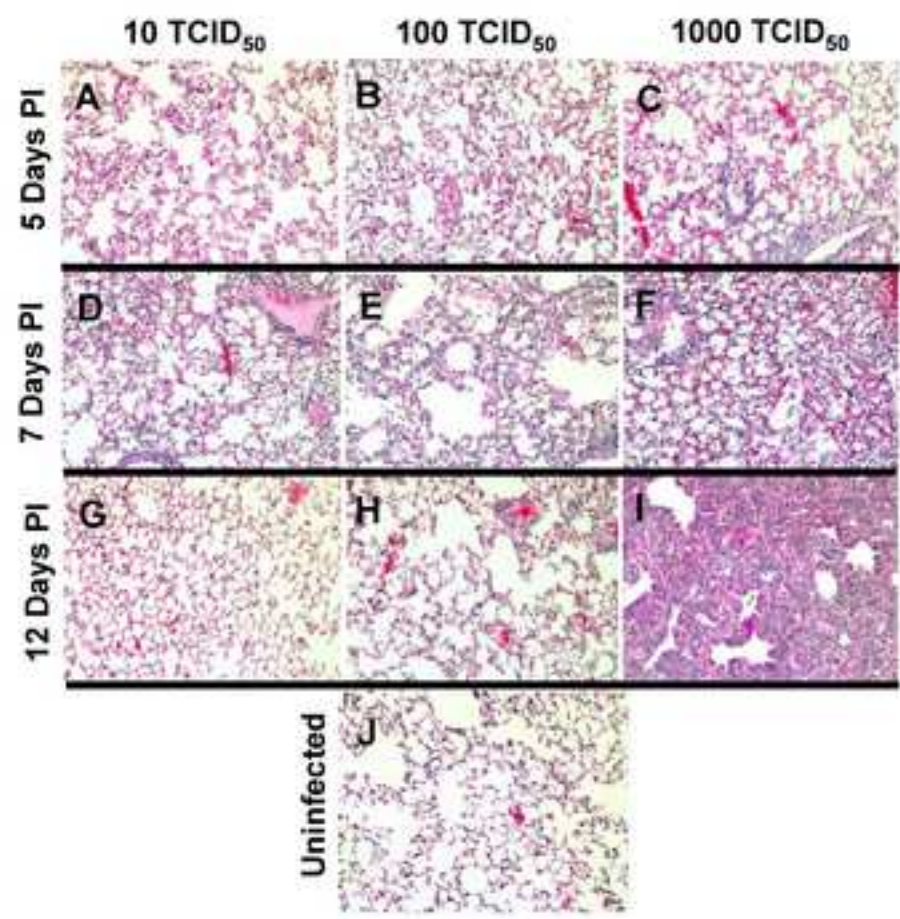


Figure 3
Verhoeven, et al

